International Journal of Applied Mechanics
Vol. 1, No. 3 (2009) 469–482

ICP Imperial College Press
www.icpress.co.uk

ACTION-DERIVED *AB INITIO* MOLECULAR DYNAMICS

S. JUN,* S. PENDURTI,† I.-H. LEE,‡ S. Y. KIM,§ H. S. PARK§
and Y.-H. KIM¶

*Department of Mechanical Engineering, University of Wyoming
Dept. 3295, 1000 E. University Avenue
Laramie, WY 82071, USA

†ASE Technologies Inc., Cincinnati, OH 45246, USA

‡Korea Research Institute of Standards and Science (KRISS)
Daejeon 305-600, Korea

§Department of Mechanical Engineering, University of Colorado
Boulder, CO 80309, USA

¶National Renewable Energy Laboratory, Golden, CO 80401, USA
*sjun@uwyo.edu

Received 11 May 2009
Accepted 19 May 2009

Action-derived molecular dynamics (ADMD) is a numerical method to search for minimum-energy dynamic pathways on the potential-energy surface of an atomic system. The method is based on Hamilton's least-action principle and has been developed for problems of activated processes, rare events, and long-time simulations. In this paper, ADMD is further extended to incorporate *ab initio* total-energy calculations, which enables the detailed electronic analysis of transition states as well as the exploration of energy landscapes. Three numerical examples are solved to demonstrate the capability of this action-derived *ab initio* molecular dynamics (MD). The proposed approach is expected to circumvent the severe time-scale limitation of conventional *ab intio* MD simulations.

Keywords: Molecular dynamics; least-action principle; *ab initio* calculations; transition pathways; activation energy.

1. Introduction

A quantitative understanding of molecular-level mechanism is often essential for predictive modelling and simulation of macroscopic properties of materials. Together with cutting-edge experimental tools of characterisation, novel multiscale modelling and simulation techniques that accommodate disparate time and length scales can have a synergistic impact on the design and control for various materials and chemical processes. Molecular dynamics (MD) has been one of the most popular

*Corresponding author.

and reliable numerical techniques for materials modelling with atomic detail, where the continuous increase in computational power has enabled large-scale MD simulations for systems of more than several billion atoms.

Nevertheless, MD still suffers from limitations of time scales. Its simulation process is basically the time-marching sequence of explicitly solving Newton's equations of motion at every discretised time step. The temporal increment is usually on the order of a femtosecond because it has to sufficiently capture the smallest dynamical phenomenon, i.e. the vibration of each atom. Otherwise, the simulation becomes numerically unstable, and blows up rapidly. Such a small time step prohibits us from expanding the physical time scale that an entire MD simulation can span. As a consequence, most MD simulations, either empirical or *ab initio*, cannot exceed a time scale of more than a few microseconds even when using the world's fastest computer. A variety of nanoscale phenomena are activated processes and/or rare events of multiple time scales, such as structural/phase transitions, defect generation and propagation, diffusion of atoms and defects, catalytic reaction, etc. Therefore, it is a central issue of computational nanoscience and technology to seek a new numerical approach that can substantially increase the time scales that are accessible while still preserving the detailed molecular-level mechanism.

In order to resolve such time-scale limitations of MD, Passerone and Parrinello [2001] and Passerone *et al.* [2003] proposed a new methodology that indirectly searches for the approximate solution of Newton's equations of motion. The method, termed action-derived molecular dynamics (ADMD), is based on Hamilton's least-action principle which is theoretically equivalent to Newton's equations of motion. By minimising the action of an atomic system, this method seeks a minimum-energy dynamic pathway on the potential-energy surface, connecting the given initial and final atomic configurations of any slow-mode or rare-event system. ADMD involves the time parameter in integral form only. It does not require the derivatives with respect to time. No explicit temporal increment is thus necessary in the formulation. As long as we are able to develop an efficient numerical algorithm to implement into the least-action principle, the method is free from any limitation of time scale, while the resulting evolution of a system basically represents the Newtonian dynamics.

Over the past several years, ADMD has been used for diverse multiple time-scale problems of rare events, activated processes and slow-mode systems, including structural transformations of carbon fullerenes [Kim *et al.*, 2003; Lee *et al.*, 2003, 2004a, 2006] and nanotubes [Kim *et al.*, 2006], conformational changes of organic molecules [Lee *et al.*, 2005], dislocation dynamics [Pendurti *et al.*, 2006], atomic diffusions on metal surfaces [Lee *et al.*, 2004b; Kim *et al.*, 2007a, b, c], and so on. However, most of these ADMD applications have only employed classical potentials or tight-binding method to represent the atomic interactions. To our knowledge, the only exception is a quantum chemical ADMD calculation for very small molecules with less than 20 atoms [Aktah *et al.*, 2004]. In order to extend the capability of ADMD for the electronic-level analysis of larger material systems, we develop in

this paper the advanced ADMD that incorporates density-functional *ab initio* total-energy calculations into its algorithm. This approach is expected to substantially extend the physical time scales that current conventional *ab initio* MD simulations can facilitate.

This paper is presented as follows. In the next section, the basic features of ADMD are briefly reviewed. Algorithm and approximation options to implement the density-functional software, SIESTA, into the framework of ADMD is described in Sec. 3. Three model problems are solved in Sec. 4 to demonstrate the capability of the proposed action-derived *ab initio* MD. Finally, concluding remarks complete the paper.

2. Brief Review of ADMD

In what follows, a very brief description on the theoretical background of ADMD is presented. A detailed introductory review can be found elsewhere [Lee *et al.*, 2004b]. For a system consisting of N number of atoms, the action (S) is defined as the time integration of its Lagrangian (L) as $S = \int_o^\tau L dt$. By discretising the entire time domain into an arbitrary number (P) of temporal intervals, we can express the discretised action (S^h) in terms of atomic positions ($\{\mathbf{q}\}$) as

$$S^h = \sum_{j=0}^{P-1} \Delta \left[\sum_{I=1}^{N} \frac{m_I}{2\Delta^2} (\mathbf{q}_j^I - \mathbf{q}_{j+1}^I)^2 - V(\{\mathbf{q}_j\}) \right], \tag{2.1}$$

where m_I is the atomic mass, V is the potential energy and Δ denotes the time interval. Unlike Newton's equations of motion, there is basically no stability-related restriction in selecting the size of time increment Δ, which makes this approach free from time-scale limitations, even though accuracy will still depend upon the size of Δ, i.e. the temporal resolution.

Given initial and final configurations (i.e. $j = 0$ and $j = P$), the stationary condition $\delta S = 0$ of the least-action principle results in a set of linear equations, and by solving it, a collection of the atomic positions $\{\mathbf{q}\}$ can be determined for all atoms ($I = 1, \ldots, N$) at all time steps ($j = 1, \ldots, P-1$). The converged solution is the dynamic pathway in configuration space for the atomic system that evolves from the given initial to final state. Throughout the entire procedure, the physical time is preserved, and dynamic phenomena of any time period can be reproduced in principle.

Unfortunately, the numerical minimisation of the above action is impractical because the extremum condition does not always mean its minimum and the pool of possible pathways is not bounded in this multidimensional configuration space. In order to circumvent this difficulty, ADMD presented a practical idea that can effectively narrow down pathway candidates by imposing strong constraints on the objective function (i.e. the discretised action). Two constraints have been realised

based on the principles of dynamics. The modified action is accordingly given as

$$\Theta(\{\mathbf{q}_j\}; E, T) = S^h + \mu_E \sum_{j=0}^{P-1} (E_j - E)^2 + \mu_K \sum_{I=1}^{N} \left(\langle K_I \rangle - \frac{3k_B T}{2} \right)^2, \qquad (2.2)$$

where k_B is the Boltzmann constant, E_j is the total energy of the system at time index j and K_I denotes the kinetic energy of Ith atom. The second term of the right-hand side imposes the conservation of total energy [Passerone and Parrinello, 2001], and the third term is to implement the virial theorem [Lee *et al.*, 2003]. For nonequilibrium processes, T is not a thermodynamic temperature but a parameter that controls the kinetic energy of the entire system [Lee *et al.*, 2003]. In practice, by finding empirically the optimised penalty parameters (μ_E and μ_K), these two extra terms can greatly enhance the pathway-searching performance for atomic systems that undergo complex structural changes.

In *ab initio* MD, the interaction between atoms is computed by *ab initio* calculations, but the time evolution of atomic positions is basically governed by Newton's equations of motion under the umbrella of the Born–Oppenheimer approximation. An important question may arise: is the resulting pathway really the solution of Newton's equations of motion? To validate it, ADMD can use a so-called error estimator by comparing the converged pathway with the Verlet trajectory that is the solution of Newton's equations of motion [Verlet, 1967; Elber *et al.*, 2003]. This verification is quantified by the Onsager–Machlup (OM) action [Onsager and Machlup, 1953] given as

$$S_{OM}^h = \sum_{I=1}^{N} \sum_{j=1}^{P-1} \left[2\mathbf{q}_j^I - \mathbf{q}_{j-1}^I - \mathbf{q}_{j+1}^I - \frac{\Delta^2}{m_I} \frac{\partial V(\{\mathbf{q}_j\})}{\partial \mathbf{q}_j^I} \right]. \qquad (2.3)$$

Direct minimisation of the OM action is intractable because it requires the second derivatives of potential energy. But, we can evaluate the OM action itself for the assessment of the final results. The OM action must be zero for an exact Verlet trajectory. The discretised action is minimised until this OM action reaches a sufficiently small value, which implies the resulting path is a good approximation to Newton's equations of motion. A systematic study has been performed by investigating the dependence of path quality upon the constraint terms added in the action, and confirmed its feasibility through the example of the Stone–Wales (SW) transformation in a fullerene [Lee *et al.*, 2003].

3. Integration of *Ab Initio* Methods with ADMD

ADMD seeks dynamic pathways of an N-atom system that evolves with respect to time. The pathway is discretised by $P+1$ images (i.e. time indices) including initial and final configurations. The computing procedure is therefore a function minimisation with $3N(P-1)$ degrees of freedom. The most time-consuming part of an MD simulation is the calculation of energy and forces. Fortunately, these calculations

can be performed independently per each image without any data communication between them. For example, computations of force and energy for a 128 time-step pathway can be performed concurrently on 128 slave nodes without any data communication between them. The message-passing interface (MPI) based parallelisation is therefore a natural choice for substantial efficiency improvement. As shown in the flowchart of ADMD (Fig. 1), the calculation of energy and force is a single module that is simultaneously called by individual time index, which enables high-performance parallel computing of the method. Numerical examples presented in the following section were computed on a Opteron Linux cluster.

This parallel structure of ADMD program makes the combination of ADMD with *ab initio* calculation very straightforward, as well. Only this force/energy calculation module is replaced by any of *ab initio* programs for the calculation of electronic

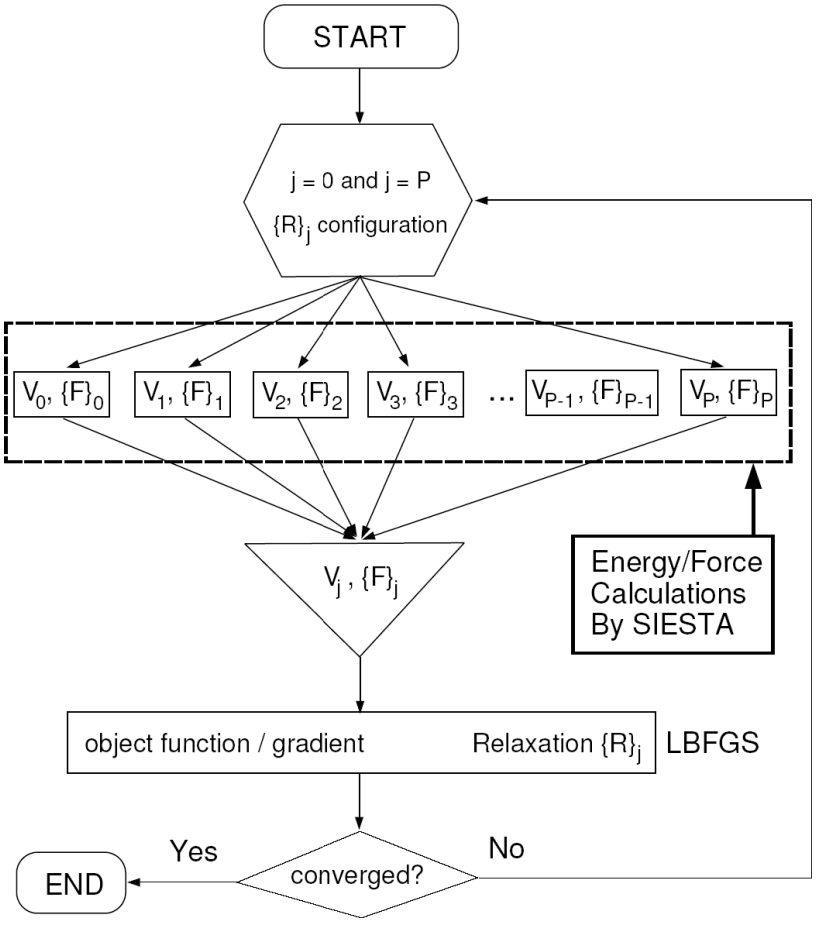

Fig. 1. Typical flowchart of action-derived molecular dynamics shows the parallel architecture for the computation of energy and force. In this paper, the module of energy and force computations is performed by the density-functional *ab initio* total-energy calculation software, SIESTA.

ground state energy and Hellmann–Feynman forces. No other part in the main program needs to be modified. We utilised the Python script for the interfacing between *ab initio* calculation program and our in-house ADMD code.

For *ab initio* total-energy calculations of the following numerical examples, we used the program SIESTA [Soler *et al.*, 2002] that implements the pseudopotential approximation and the basis set of numerical atomic orbitals [Goedecker, 1999; Kim *et al.*, 1995; Mauri *et al.*, 1993; Ordejón, 1998; Ordejón *et al.*, 1993] into the framework of density-functional theory [Hohenberg and Kohn, 1964; Kohn and Sham, 1965]. The norm-conserving nonlocal Troullier–Martins pseudopotential [Troullier and Martins, 1991], factorized in the Kleinman–Bylander separable form [Kleinman and Bylander, 1982], was employed. We employed local density approximation (LDA) by using the Ceperley–Alder exchange-correlation functional [Ceperley and Alder, 1980] as parameterised by Perdew and Zunger [1981]. A basis set of double-ζ plus polarisation functions was used for the valence electrons of carbon atom with the energy shift parameter of 0.02 Ry [Artacho *et al.*, 1999; Soler *et al.*, 2002]. An energy cutoff of 100 Ry was set for the real-space integrations. The relaxed atomic positions were obtained by the conjugate gradient optimisation until the forces on each atom were smaller than 0.02 eV/Å.

4. Numerical Examples

4.1. *SW transformation in a carbon fullerene*

As the first demonstration example of the action-derived *ab initio* MD, we simulated the SW transformation in a C_{60} fullerene where a C–C bond rotates 90° with respect to the midpoint of the bond. The SW bond rotation is not only a unit process of various structural transformation of carbon networks, but also responsible for their mechanical properties such as the brittle–ductile transitions in carbon nanotubes (CNTs).

We discretised the entire process into 101 images including the initial and final states. This discretisation is sufficient to resolve the activated complex in the vicinity of the transition state along the minimum-energy dynamic pathway. Figure 2 shows the results of energy profiles along with the atomic structure and total charge density of the transition state. The breaking of two C–C bonds is clearly shown in the charge density plot. The energy difference between the fully relaxed initial and final configurations is 1.554 eV that agrees well with the result (1.55 eV) of a density-functional calculation by generalised gradient approximation (GGA) [Bettinger *et al.*, 2003]. We obtained the energy barrier of 7.744 eV. This LDA calculation is slightly higher than GGA density-function *ab intio* total-energy calculations (6.91–7.35 eV), while it is lower than the results of an modified neglect of differential overlap (MNDO) semi-empirical method (8.5 eV) and a GGA/MNDO hybrid calculation (8.1 eV) [Bettinger *et al.*, 2003].

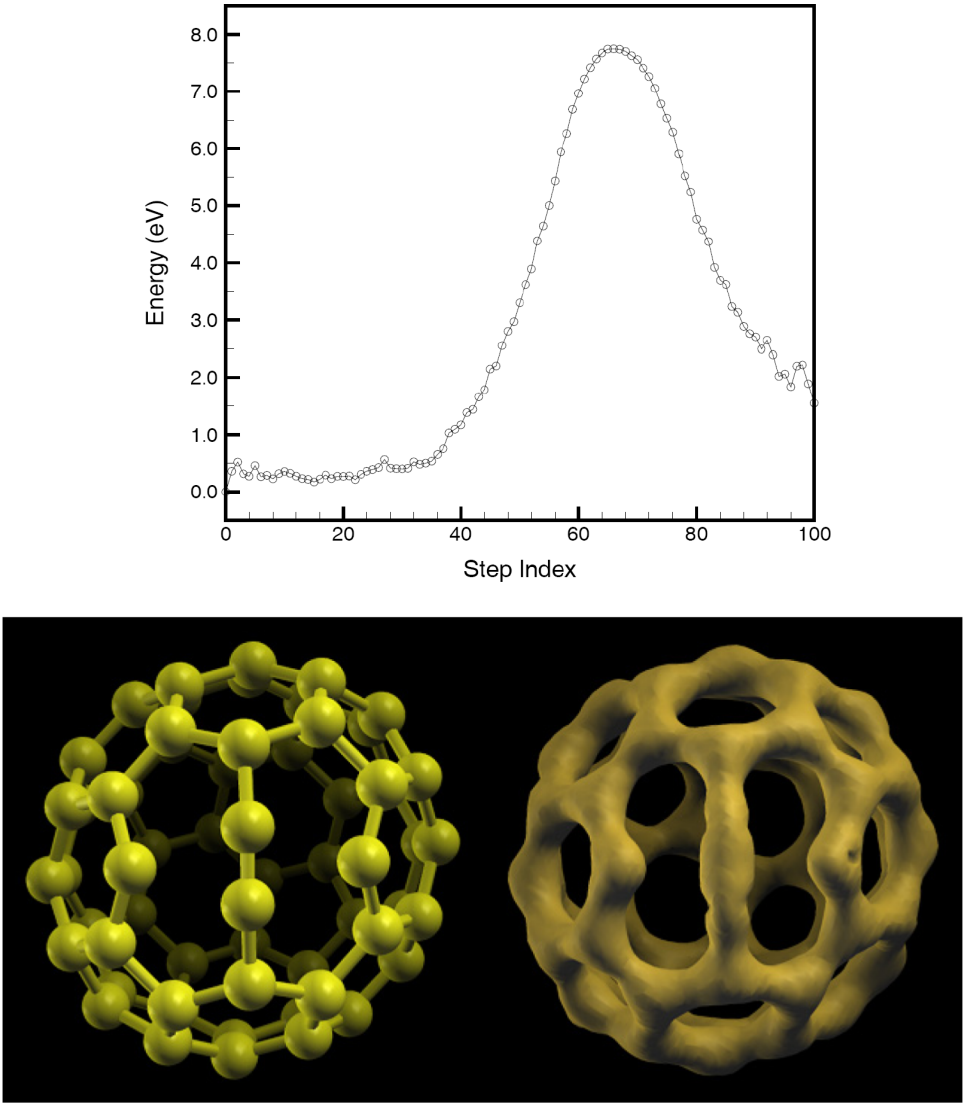

Fig. 2. The Stone–Wales transformation in a C_{60} fullerene. Top: Energy profile along the transition pathway. The energy barrier is 7.744 eV. Bottom left: Atomic configuration of the transition state. Bottom right: Isosurface of the total charge density of the transition state.

4.2. *Diffusion of noble gas atoms through graphene monolayer*

Recently, Bunch *et al.* [2008] experimentally demonstrated that a graphene membrane can separate two regions filled with different gases and respond to the resulting pressure differences. They did not detect any leakage of gas atoms through the graphene sheet, which indicates its promise as an ideal, ultrasensitive impermeable membrane and pressure sensor. Understanding whether a noble gas atom of small

atomic radius can easily pass through a carbon ring in graphene is essential for the design of such graphene-based pressure sensors integrated in NEMS. The second demonstration example of the action-derived *ab initio* MD is the diffusion of light noble gas atoms (He and Ne) through a graphene monolayer.

The graphene model consists of 24 carbon atoms placed in a fully periodic 3D supercell. The out-of-plane height of the supercell (i.e. vacuum zone) is 10 Å so that the interaction between layers can be neglected. We initially placed a gas atom above the graphene layer; the projected in-plane locations of the noble gas atoms corresponded to the centre of a hexagonal ring in the graphene. The distance from the graphene layer to the He and Ne atoms are 2.818 and 2.931, respectively. Since the current *ab initio* approach does not account for van der Waals interactions, these initial distances between the gas atoms and graphene layer were adopted from the energy minimisations using empirical potentials incorporating the van der Waals interaction [Kim *et al.*, in preparation].

For each noble gas atom, two diffusion paths were examined as shown in Fig. 3. The first path (path A) is a straight downward diffusion route for which the projected in-plane positions of the gas atom in the initial and final configurations were set identical. For this case, the atom vertically penetrates graphene along the centre of the hexagon ring. The second path (path B) is an inclined pathway where the initial and final projected in-plane positions of the diffusing atom are not the same. The final projected position is the centre of the neighbouring hexagon ring. Therefore, the atom diffuses down toward a C–C bond shared by these two hexagon rings, breaks the bond and then moves further down to the designated final position.

Figure 3 also shows the energy profiles of the two diffusion paths for He atom. Both paths were discretised by 41 images. It is noted that the simulation time is not the same for these two paths because path B takes longer time. Nevertheless, the results are compared using the same x-axis of time step, for convenience. The energy barriers of paths A and B are, respectively, 9.528 and 10.668 eV. The transition states for both pathways are given in Fig. 4. While path B shows the breaking of the targeted C–C bond, the He atom of path A simply passes through the hexagon ring without any bond breaking. Therefore, it is clear that path B demands higher energy to take place.

However, Ne diffusion reveals opposite results. As shown in Fig. 5, the energy barrier of path B is much lower than that of path A. The transition states for both pathways are shown in Fig. 6. As opposed to He cases, strong repulsive interaction between He and carbon atoms of path A drives the breaking of two C–C bonds, while only the targeted C–C bond is broken in path B. Total charge density plots in Fig. 6 verify it. Accordingly, the energy barriers of path A (21.316 eV) is much higher than the activation energy of path B (13.390 eV).

Even though this demonstration example is quantitative rather than rigorous, the interesting difference between He and Ne cases can motivate more qualitative study of permeable diffusion of gases through graphene membranes. With this

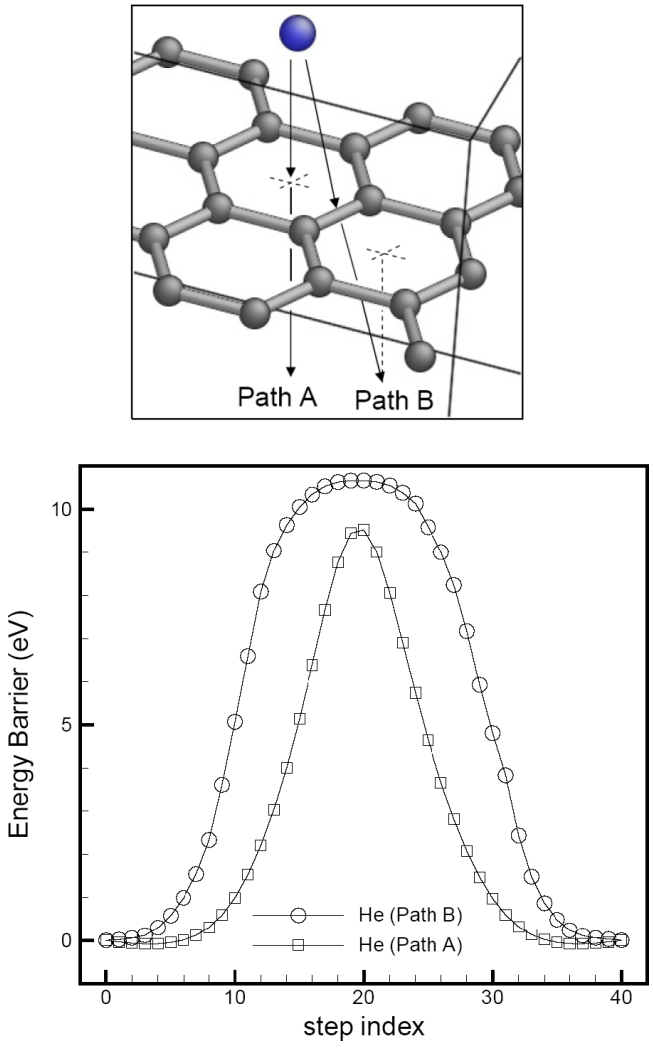

Fig. 3. Permeable diffusion of a He atom through a graphene monolayer. Top: Two presumed diffusion paths are considered. Bottom: Energy plots of the two diffusion paths.

numerical technique, unexpected low-energy diffusion pathways can possibly be found by larger sizes of graphene model with a variety of gas atoms and molecules. In addition, for more accurate description of atomic interaction, the van der Waals interaction should be implemented into the *ab initio* method employed.

4.3. *Fundamental mechanism of silicon carbide nanotube synthesis*

The last numerical example of the action-derived *ab intio* MD concerns the basic mechanism of SiC nanotube synthesis. The simulation was motivated by the recent work of Sun *et al.* [2002], in which the SiC nanotubes were formed by reacting CNTs

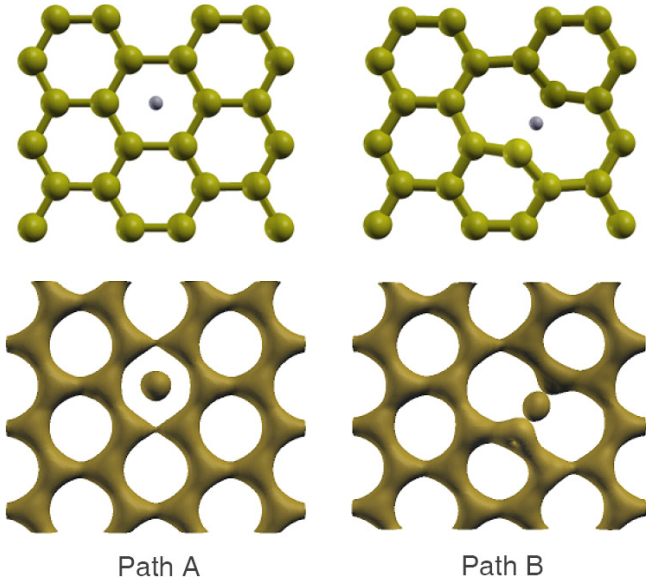

Fig. 4. Permeable diffusion of a He atom through a graphene monolayer. Transition states of the two diffusion mechanisms: (top) atomic configuration and (bottom) isosurface of total charge density.

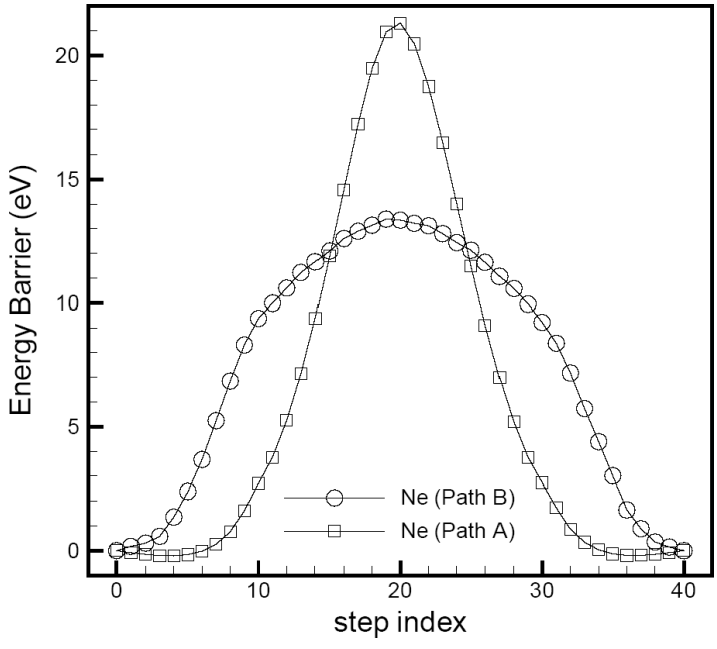

Fig. 5. Permeable diffusion of a Ne atom through a graphene monolayer. Energy plots of the two diffusion paths.

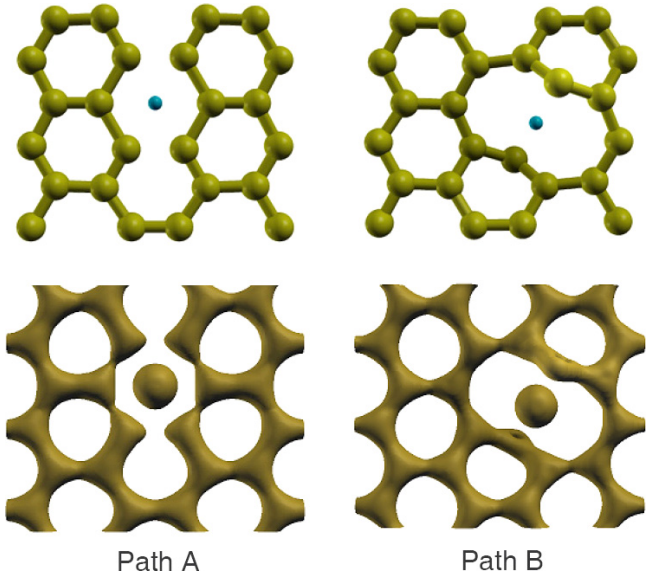

Fig. 6. Permeable diffusion of a Ne atom through a graphene monolayer. Transition states of the two diffusion mechanisms: (top) atomic configuration and (bottom) isosurface of total charge density.

with SiO at elevated temperatures, leading to a multi-walled nanotube structure of which the outer nanotube was SiC. We present here *ab initio* ADMD simulation result of the very beginning stage out of the entire process with relatively simple model.

In the initial configuration, we considered a SiO molecule placed above a graphene layer model consisting 60 carbon atoms with periodic boundary condition. On the other hand, in our final configuration, we have a CO molecule above

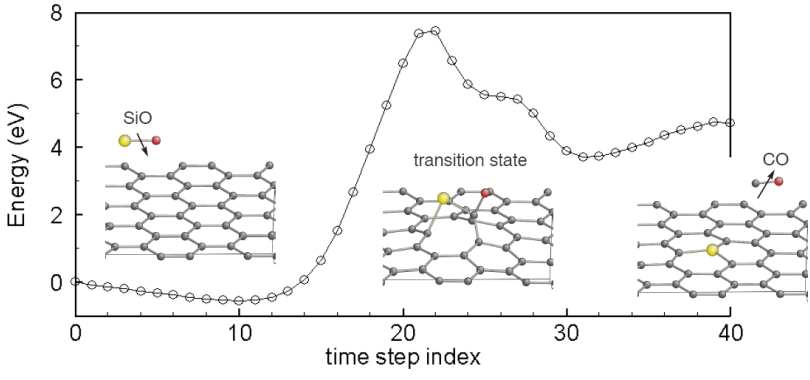

Fig. 7. Basic process of SiC nanotube synthesis. A SiO molecule interacts with graphene monolayer to replace C by Si. The carbon atom binds with the oxygen atom to make a CO molecule and leaves the Si embedded carbon network. The calculated activation energy is 7.999 eV.

the graphene in which one carbon atom was replaced by the Si atom. Then, the minimum-energy reaction pathway connecting these two configurations is calculated by the action-derived *ab intio* MD. The schematic process of this reaction is given in Fig. 7 together with the computed result of potential-energy variation. Selected

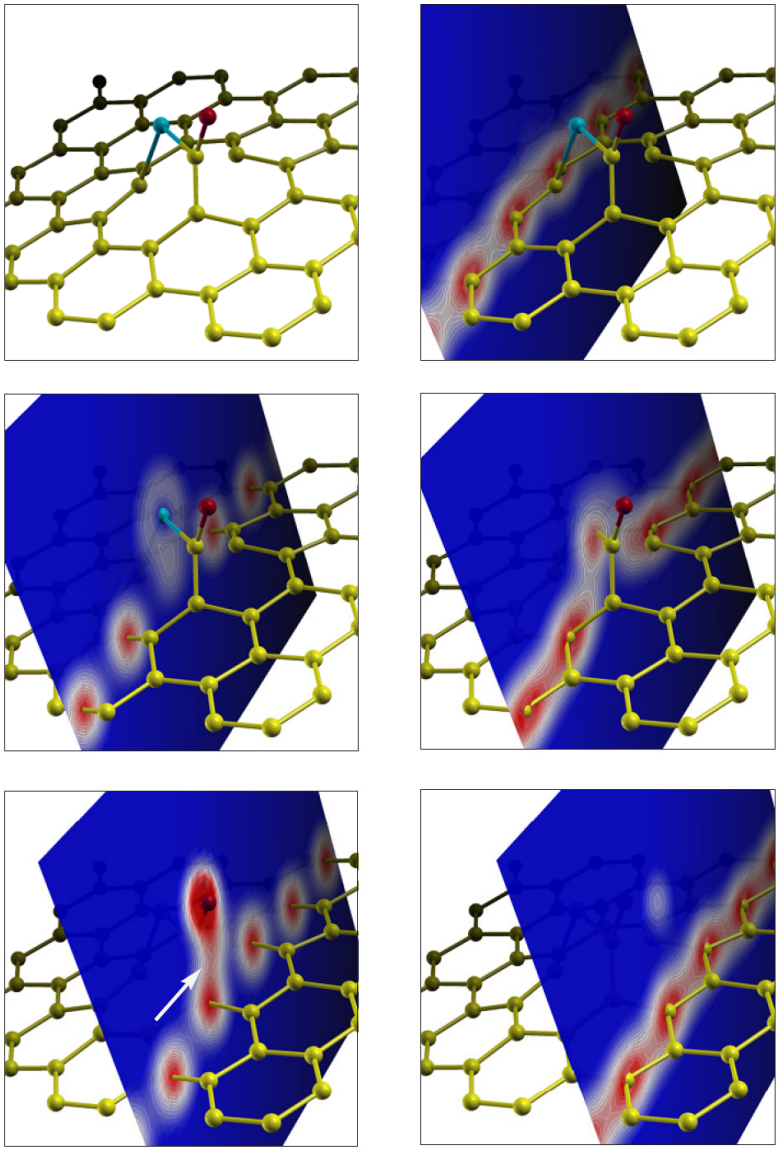

Fig. 8. The transition state of the replacement process. The upper left panel is for the atomic configuration of the transition state. Others are for its total charge density contours on selected planes. Si (blue) already makes strong bonding with two carbon (gold) atoms, one of which also binds with O (red). A weak bonding between oxygen and the other graphene atom is also found.

total charge density profiles of the transition state are shown in Fig. 8. The obtained energy barrier is 7.999 eV. This value is comparable with the activation energy of the bond rotation in a C_{60} fullerene. In general, the SW transformation requires much higher activation energy in graphene (more than 10 eV) than in a fullerene. However, the above SiO-to-CO reaction takes place with considerably lower energy barrier.

From the analysis of total charge density at the transition state, it is found that, in addition to forming a CO molecule, the oxygen atom forms a weak bond with other carbon atoms in graphene (see the white arrow in Fig. 8). On the other hand, the bonds between Si and O are completely broken and Si binds with two graphene atoms at the transition state. This example well demonstrates that we can perform detailed electronic analysis of transition states of complex chemical reactions using the action-derived *ab initio* MD, as well as the searching of minimum-energy dynamic pathways.

5. Concluding Remarks

We have presented a numerical approach that integrates ADMD with *ab intio* total-energy calculation. Based on Hamilton's least-action principle, ADMD seeks minimum-energy dynamic pathways on potential-energy surface. This method is very useful for problems of activated processes, rare events and long-time simulations, overcoming the time-scale limitation of conventional MD. In this paper, we extended the method to link with a density-functional *ab initio* software, SIESTA. This new approach enables not only the detailed electronic analysis of transition states but also long-time simulation of *ab initio* MD. Through the numerical examples, we have demonstrated this capability of the action-derived *ab initio* MD. The proposed approach is expected to circumvent the severe time-scale limitation of conventional *ab intio* MD simulations.

Acknowledgements

The work of SJ was made possible in part by NIH Grant # P20 RR016474 from the INBRE Program of the National Centre for Research Resources. Its contents are solely the responsibility of the author and do not necessarily represent the official views of NIH. SYK and HSP both gratefully acknowledge the support of DARPA through Grant HR0011-08-1-0047. The authors note that the content of this article does not necessarily reflect the position or the policy of the government, and that no official government endorsement of the results should be inferred. HSP also acknowledges support from NSF Grant CMMI-0750395.

References

Aktah, D., Passerone, D. and Parrinello, M. [2004] *J. Phys. Chem. A* **108**, 848.

Artacho, E., Sánchez-Portal, D., Ordejón, P., García, A. and Soler, J. M. [1999] *Phys. Status Solidi B* **215**, 809.

Bettinger, H. F., Yakobson, B. I. and Scuseria, G. E. [2003] *J. Am. Chem. Soc.* **125**, 5572.
Bunch, J. S., Verbridge, S. S., Alden, J. S., van der Zande, A. M., Parpia, J. M., Craighead, H. G. and McEuen, P. L. [2008] *Nano Lett.* **8**, 2458.
Ceperley, D. M. and Alder, B. J. [1980] *Phys. Rev. Lett.* **45**, 566.
Elber, R., Cárdenas, A., Ghosh, A. and Stern, H. A. [2003] *Adv. Chem. Phys.* **126**, 93.
Goedecker, S. [1999] *Rev. Mod. Phys.* **71**, 1085.
Hohenberg, P. and Kohn, W. [1964] *Phys. Rev. B* **136**, B864.
Kim, J., Mauri, F. and Galli, G. [1995] *Phys. Rev. B* **52**, 1640.
Kim, Y.-H., Lee, I.-H., Chang, K. J. and Lee, S. [2003] *Phys. Rev. Lett.* **90**, 65501.
Kim, S. Y., Lee, I.-H., Jun, S., Lee, Y. and Im, S. [2006] *Phys. Rev. B* **74**, 195409.
Kim, S. Y., Lee, I.-H. and Jun, S. [2007a] *Phys. Rev. B* **76**, 245407.
Kim, S. Y., Lee, I.-H. and Jun, S. [2007b] *Phys. Rev. B* **76**, 245408.
Kim, S. Y., Lee, I.-H. and Jun, S. [2007c] *Int. J. Multiscale Comput Eng.* **5**, 273.
Kim, S. Y., Jun, S. and Park, H. S. [2008] in preparation.
Kleinman, L. and Bylander, D. M. [1982] *Phys. Rev. Lett.* **48**, 1425.
Kohn, W. and Sham, L. J. [1965] *Phys. Rev.* **140**, A1133.
Lee, I.-H., Lee, J. and Lee, S. [2003] *Phys. Rev. B* **68**, 64303.
Lee, I.-H., Kim, H. and Lee, J. [2004a] *J. Chem. Phys.* **120**, 4672.
Lee, I.-H., Kim, S. Y. and Jun, S. [2004b] *Comput. Meth. Appl. Mech. Eng.* **193**, 1633.
Lee, I.-H., Kim, S.-Y. and Lee, J. [2005] *Chem. Phys. Lett.* **412**, 307.
Lee, I.-H., Jun, S., Kim, H., Kim, S. Y. and Lee, Y. [2006] *Appl. Phys. Lett.* **88**, 011913.
Mauri, F., Galli, G. and Car, R. [1993] *Phys. Rev. B* **47**, 9973.
Onsager, L. and Machlup, S. [1953] *Phys. Rev.* **91**, 1505.
Ordejón, P. [1998] *Comput. Phys. Commun.* **12**, 157.
Ordejón, P., Drabold, D. A., Grumbach, M. P. and Martin, R. M. [1993] *Phys. Rev. B* **48**, 14646.
Passerone, D. and Parrinello, M. [2001] *Phys. Rev. Lett.* **87**, 108302.
Passerone, D., Ceccarelli, M. and Parrinello, M. [2003] *J. Chem. Phys.* **118**, 2025.
Pendurti, S., Jun, S., Lee, I.-H. and Prasad, V. [2006] *Appl. Phys. Lett.* **88**, 201908.
Perdew, J. P. and Zunger, A. [1981] *Phys. Rev. B* **23**, 5048.
Soler, J., Artacho, E., Gale, J. D., García, A., Junquera, J., Ordejón, P. and Sánchez-Portal, D. [2002] *J. Phys.: Condens. Matter* **14**, 2745.
Sun, X.-H., Li, C.-P., Wong, W.-K., Wong, N.-B., Lee, C.-S., Lee, S.-T. and Teo, B.-K. [2002] *J. Am. Chem. Soc.* **124**, 14464.
Troullier, N. and Martins, J. L. [1991] *Phys. Rev. B* **43**, 1993.
Verlet, L. [1967] *Phys. Rev.* **159**, 98.